Check for updates

Received: 8 August 2022 | Revised: 27 June 2023 | Accepted: 3 July 2023

DOI: 10.1002/joc.8180

RESEARCH ARTICLE

International Journal of Climatology RMetS

An analysis of the spatial variation of tropical cyclone rainfall trends in Mainland Southeast Asia

Aifang Chen[1] | **Hao Huang**[1] | **Jie Wang**[2] | **Yuxin Li**[1] | **Deliang Chen**[3] | **Junguo Liu**[1,4]

[1]School of Environmental Science and Engineering, Southern University of Science and Technology, Shenzhen, China

[2]College of Earth and Environmental Sciences, Lanzhou University, Lanzhou, China

[3]Regional Climate Group, Department of Earth Sciences, University of Gothenburg, Gothenburg, Sweden

[4]Henan Provincial Key Laboratory of Hydrosphere and Watershed Water Security, North China University of Water Resources and Electric Power, Zhengzhou, China

Correspondence
Junguo Liu, School of Environmental Science and Engineering, Southern University of Science and Technology, Shenzhen 518055, China.
Email: junguo.liu@gmail.com

Funding information
China Postdoctoral Science Foundation, Grant/Award Number: 2021M691403; National Natural Science Foundation of China, Grant/Award Numbers: 91537210, 42101041; the Henan Provincial Key Laboratory of Hydrosphere and Watershed Water Security; the SUSTech Presidential Postdoctoral Fellowship; Strategic Priority Research Program of the Chinese Academy of Sciences, Grant/Award Numbers: XDA20060401, XDA20060402; Swedish STINT, Grant/Award Number: CH2019-8377

Abstract

Tropical cyclones (TCs) and the associated rainfall (TCR) have received increasing attention because of their catastrophic damages. Due to the differences in TC characteristics and TCR in different ocean basins, the changes in TCR would be complicated for areas receiving TC landfalling from multi-basins. Therefore, separating TCR and TC characteristics from the formation basins can offer more insights for accurately evaluating TCR in the landfalling areas. Here we selected the TC-prone Mainland Southeast Asia (MSEA) to investigate changes in TCR regarding TC characteristics from the surrounding formation basins from 1983 to 2020. Results show that the interannual variability of the total TCs influencing MSEA (MSEA-ALL-TC) characteristics, including number, total duration, maximum intensity and accumulated cyclone energy, was dominated by the TCs originating from the Western North Pacific (WNP-TC). However, the total TCR was controlled by the TCs originating from the WNP and the South China Sea (SCS-TC), whose influence on TCR was concentrated in the eastern MSEA. TCR associated with TCs originating from the Bay of Bengal was relatively small and concentrated in the western MSEA. For the whole MSEA, the total TCR contributed up to 47% of the annual extreme rainfall amount. Annual TCR presented significant decreasing trends in the southeast MSEA, while increasing trends exist in the northeast. These contrasting trends are attributed to the reduced tendency of WNP-TC track density and the increased SCS-TC rainfall rate. We also found that the SCS-TC induced a higher rainfall rate than the other two basins. The TC characteristics of number, total duration, maximum intensity and accumulated cyclone energy were significantly correlated with TCR in each formation basin, with the highest correlation of the total duration. This study improves our understanding of the influence of changes in TC characteristics on TCR in the TC multi-source region.

KEYWORDS

Mainland Southeast Asia, PERSIANN-CDR, tropical cyclone characteristics, tropical cyclones rainfall, tropical cyclones source basin

This is an open access article under the terms of the Creative Commons Attribution-NonCommercial-NoDerivs License, which permits use and distribution in any medium, provided the original work is properly cited, the use is non-commercial and no modifications or adaptations are made.
© 2023 The Authors. *International Journal of Climatology* published by John Wiley & Sons Ltd on behalf of Royal Meteorological Society.

1 | INTRODUCTION

Tropical cyclones (TCs) are destructive natural hazards, usually bringing extreme rainfall that is highly susceptible to triggering flash floods (Peduzzi et al., 2012; Rappaport, 2014). The modelled projection for a 2°C anthropogenic global warming indicated that the average TC intensity and rainfall rate are likely to increase by about 5% and 14%, respectively (Knutson et al., 2010, 2020; Sobel et al., 2016; Vosper et al., 2020), which make TC and the associated TC rainfall (TCR) receive increasing attention. Therefore, examining the TC and TCR changes and unravelling the contributions from the TC formation basins is critical to better mitigate TC-associated risks.

The contribution of TCR to annual total rainfall varies in global TC landfalling regions (Jiang & Zipser, 2010; Khouakhi et al., 2017; Skok et al., 2013). East Asia is one of the regions receiving considerable TCR (>400 mm/yr) (Chen & Fu, 2015; Cheung et al., 2018; Khouakhi et al., 2017; Kubota & Wang, 2009). TCR is also crucial to extreme rainfall events, contributing about 35%–60% of extreme rainfall in East Asia (Jiang et al., 2011; Khouakhi et al., 2017). Several studies have investigated the changes in the spatiotemporal distribution of TCR in East Asia, showing heterogeneous change patterns in different parts of the region. Kim et al. (2006) found a significant increase in TC-induced heavy rainfall in Korea during August–September from 1978 to 2005. Zhang et al. (2013) found that the average TCR per TC significantly increased in Southeast China from 1965 to 2009. Liu and Wang (2020) found a significant increasing trend of TCR in southeast China but a decreasing trend in south China from 1980 to 2017. Nguyen-Thi et al. (2012) found increasing TCR trends in central Vietnam from 1961 to 2008.

TCR is highly associated with TC characteristics, such as intensity, track, duration and frequency (Bakkensen et al., 2018; Cheung et al., 2018; Rappaport, 2014; Weinkle et al., 2012). TC characteristics have changed on temporal and spatial scales over the past decades (Sobel et al., 2021; Walsh et al., 2016). For example, in the Western North Pacific (WNP), there has been a north-westward shift of TCs since the 1960s (Knutson et al., 2020; Lee et al., 2012; Murakami et al., 2020; Wang & Toumi, 2021), and increasing TC rapid intensification associated with enhanced ocean surface warming from 1979 (Mei & Xie, 2016). On the other hand, in the northern South China Sea (SCS), weaker tendencies of landfalling TC intensity occurred because of shorter TC lifetimes from 1977 to 2010 (Park et al., 2014). These changes in TC characteristics could influence the TCR of the landfalling areas.

Additionally, the TCR brought from different basins would be distinctly different since the TCs generally have different originating conditions in their formation basins (Sobel et al., 2021; Walsh et al., 2016). For example, TCs originating in the WNP usually have long lifetimes and intensification periods over the ocean, allowing for long duration and strong intensity (Camargo & Sobel, 2005; Choi et al., 2019). On the other hand, the flat ocean topography of the Bay of Bengal (BoB) favours warming sea surface temperature and acceleration of TC intensity (Hoarau et al., 2012). The SCS TCs generally have short developing times because of the close genesis location to the coast, resulting in short duration and weak intensity (Park et al., 2014; Wang et al., 2007). TC frequency is also different among the basins. The WNP is the most active basin, accounting for over 30% of the global TC number; the North Indian Ocean, where the BoB belongs, produces <5% of the global TC number (Fudeyasu et al., 2014). Accordingly, changes in TCR would be more complicated for regions receiving TC landfalling from multi-basins, which suggests separating TCR and TC characteristics from the formation basins could offer more insights for the accurate evaluation of TCR in the landfalling regions.

In particular, Mainland Southeast Asia (MSEA) is often hit by TCs originating in the WNP, SCS and BoB (Figure 1). About a quarter of floods in this region during 1985–2018, causing substantial property damages and life losses, can be attributed to the TCR (Chen, Giese, & Chen, 2020; Hu et al., 2018; Liu et al., 2022). Affected by TCs from different formation basins, spatiotemporal patterns of the TCR in this region are complicated. However, existing works on the TCR in the MSEA mainly focused on the total TCR and the contributions to extreme rainfall in Vietnam, Thailand and Mekong River Basin (Chen et al., 2019; Chhin et al., 2016; Nguyen-Thi et al., 2012; Takahashi & Yasunari, 2008). Therefore, it is necessary to systematically estimate the spatiotemporal changes of TCR and the contributing TC characteristics, to disentangle the impact of TCs from the formation basins to the TCR in the MSEA. This study selected the MSEA as the study area to examine the TCR from different formation basins and the association with TC characteristics in the MSEA by utilizing the state-of-the-art best track data and satellite precipitation data.

2 | MATERIALS AND METHODS

2.1 | Materials

The latest International Best Track Archive for Climate Stewardship (IBTrACS) version 4 (https://www.ncdc.noaa.gov/ibtracs/), which is a centralized collection and distribution resource for TC best track data and provides the complete global set of historical TC data available (Knapp

10970088, 2023, 13, Downloaded from https://rmets.onlinelibrary.wiley.com/doi/10.1002/joc.8180, Wiley Online Library on [19/06/2024]. See the Terms and Conditions (https://onlinelibrary.wiley.com/terms-and-conditions) on Wiley Online Library for rules of use; OA articles are governed by the applicable Creative Commons License

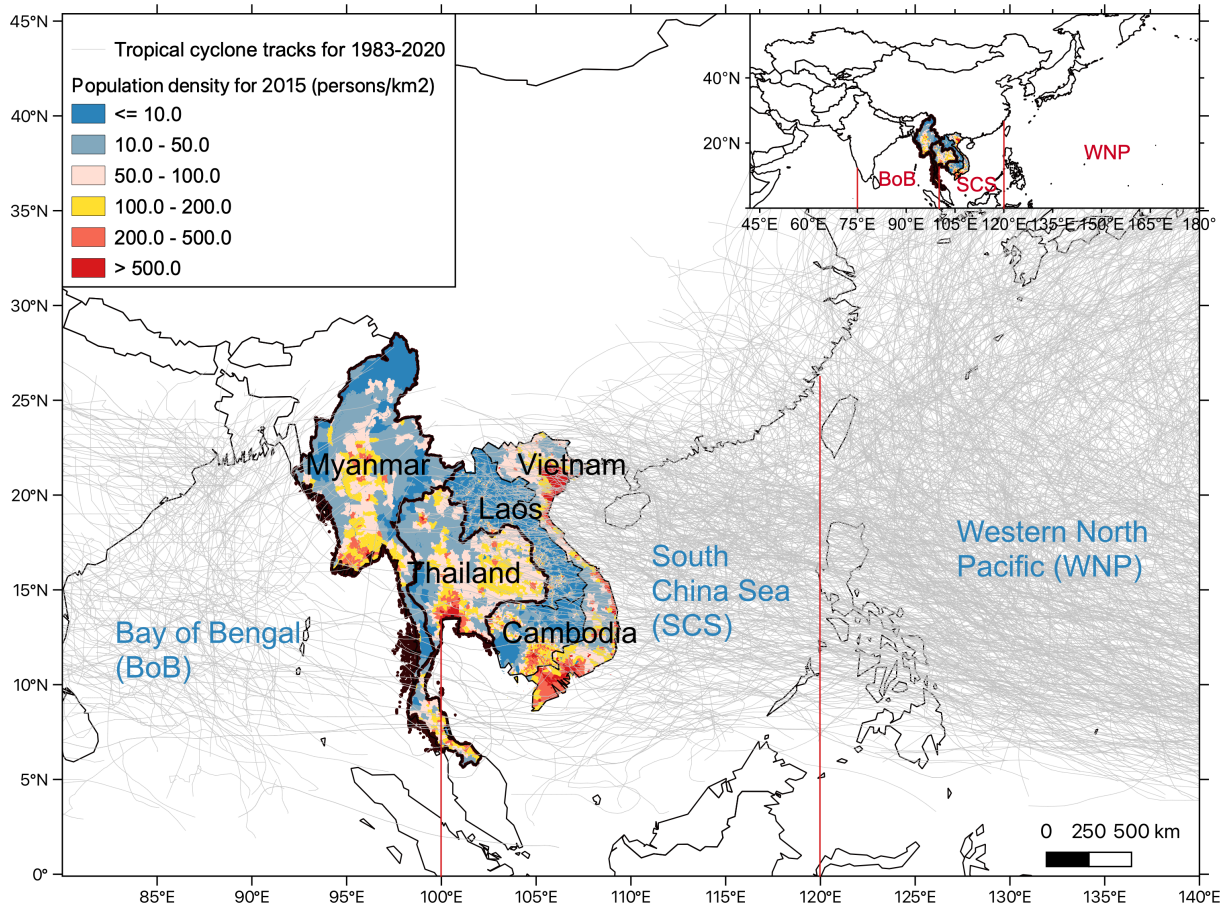

FIGURE 1 Population density in and tropical cyclone tracks over the seas surrounding Mainland Southeast Asia. The boundaries of the WNP, SCS and BoB are marked in red lines. The population density data for 2015 is from the Gridded Population of the World, Version 4 (GPWv4) (https://sedac.ciesin.columbia.edu/data/set/gpw-v4-population-count-rev11); the tropical cyclone tracks for 1983–2020 are from the latest International Best Track Archive for Climate Stewardship (IBTrACS) version 4 (https://www.ncdc.noaa.gov/ibtracs/). [Colour figure can be viewed at wileyonlinelibrary.com]

et al., 2010; Walsh et al., 2016). Since the precipitation data is available from 1983, we employed the TC track data for 1983–2020 from the IBTrACS obtained from the United States agencies, including the Joint Typhoon Warning Center, the National Hurricane Center and the Central Pacific Hurricane Center, which monitor the TCs originating in the formation basins (Emanuel, 2005). Due to the uncertainties in low-intensity storms, we only considered the TCs with a maximum intensity >34 knots (kt; Lee et al., 2012). According to the depiction of the IBTrACS and previous studies, the WNP, SCS and BoB basins are in the Northern Hemisphere with latitude >0°N, and the longitude boundaries are defined as 120°–180°E, 100°–120°E and 78°–100°E, respectively (Goh & Chan, 2010; Knapp et al., 2010; Lee et al., 2012). TCs formed within these defined boundaries are considered as originating in the respective basins. TCs from WNP, SCS and BoB were abbreviated as WNP-TC, SCS-TC and BoB-TC, respectively; and the total TCs of these three basins that influenced the MSEA were abbreviated as MSEA-ALL-TC. As a result, 356 TCs in total influenced or made landfall in the MSEA during 1983–2020 (hereafter referred to as landfalling TCs).

Considering the rare and sparse ground observations in the MSEA (Chen et al., 2018), we employed rainfall data from the Precipitation Estimation from Remotely Sensed Information using Artificial Neural Networks-Climate Data Record (PERSIANN-CDR, https://www.ncdc.noaa.gov/cdr/atmospheric/precipitation-persiann-cdr) (Ashouri et al., 2015; Sorooshian et al., 2000) to estimate TCR change in the MSEA. This data is available from 1983 to the present on the daily scale with a 0.25° horizontal resolution, which is of sufficient length, consistency, and continuity to determine climate variability and change (Ashouri et al., 2015; Chen et al., 2018; Huang et al., 2016; Liu et al., 2017). Also, it has been proven to have high accuracy in the MSEA region (Chen et al., 2018).

10970088, 2023, 13, Downloaded from https://rmets.onlinelibrary.wiley.com/doi/10.1002/joc.8180, Wiley Online Library on [19/06/2024]. See the Terms and Conditions (https://onlinelibrary.wiley.com/terms-and-conditions) on Wiley Online Library for rules of use; OA articles are governed by the applicable Creative Commons License

2.2 | Methods

To measure the change in TC activity, we used four characteristics of the TCs influencing the MSEA on the annual scale, including TC number, total duration, maximum intensity and accumulated cyclone energy (ACE). The annual TC number representing TC frequency was defined as the total number of TCs per year. The annual total duration was defined as the total duration of all TCs when influencing the MSEA in a year. The annual maximum intensity was defined as the maximum intensity of all TCs when influencing the MSEA in a year. Finally, the annual ACE is the sum of the squares of the 3-hour maximum sustained wind speed over the lifetime of all the TCs in a year (Bell et al., 2000). The annual ACE accounts for the intensity, number and duration of TCs, which is a measure of overall TC activity. Trend analysis was conducted using the conventional Sen's slope (Sen, 1968) and Mann–Kendall (Kendall, 1938) analyses. Also, Pearson correlation analysis was used to evaluate correlations between the annual TC characteristics and TCR.

To examine the climatology and trend of TCR, we investigated the annual mean and trend of TCR and the contribution of TCR to extreme rainfall. First, we considered daily rainfall as TC-induced when the rainfall occurred within a 500 km radius from the storm center (recorded by IBTrACS) during a time window of ±1 day (Chen et al., 2019; Jiang & Zipser, 2010; Kubota & Wang, 2009; Zhang, Gu, et al., 2018). Then, the annual TCR was obtained. The contribution of TCR to extreme rainfall was estimated using the peak-over-threshold (POT) method (Khouakhi et al., 2017). For each grid of the MSEA, the 95th percentile of the rainfall distribution for the rainy days across the study period was taken as the threshold. Besides, the center of gravity model (Koren et al., 2009) was employed to analyse the regional TCR center, which helped investigate changes in TCR (equation [1]). To examine the influence of TCs from the three formation basins on TCR in the MSEA, we also estimated the annual TCR and daily TC rainfall rate for MSEA-ALL-TC, WNP-TC, SCS-TC and BoB-TC, respectively.

$$\begin{cases} \overline{\mathrm{Lon}} = \dfrac{\sum_{i=1}^{n} \mathrm{Lon}_i P_i}{\sum_{i=1}^{n} P_i} \\ \overline{\mathrm{Lat}} = \dfrac{\sum_{i=1}^{n} \mathrm{Lat}_i P_i}{\sum_{i=1}^{n} P_i} \end{cases} \quad (1)$$

where $\overline{\mathrm{Lon}}$ and $\overline{\mathrm{Lat}}$ are the center of the gravity; Lon_i is the longitude of the ith pixel, Lat_i are the latitude of the ith pixel; and P_i is the TCR of the ith pixel.

We investigated the association between the TCR and TC tracks. The TC track positions reported every 3 h were transformed into the area-averaged TC track density (TCD) occurring at 1° × 1° grid box, which was smoothed by a 9-point weighted smoother (Wang et al., 2010). The TCD is a proxy reflecting both TC number and duration. We considered all TCs occurred during the study period from the WNP, SCS and BoB with maximum intensity >34 kt. The singular value decomposition (SVD) analysis was applied to examine the coupled variability of MSEA-ALL-TC's TCR and TCD (Bretherton et al., 1992). The leading modes of SVD analysis explain the dominant spatial characteristics of interannual variability, and the corresponding time series illustrates how the amplitude of such leading modes varies over time. The heterogeneous correlation coefficient was calculated to analyse the key area of the interactions between the TCR and TCD. In addition, the climatology and trend of TCD of MSEA-ALL-TC, WNP-TC, SCS-TC and BoB-TC were also investigated.

3 | RESULTS

3.1 | Statistics of TC characteristics

9.4 MSEA-ALL-TC influenced the MSEA annually during 1983–2020, with a total duration of 538.3 h, maximum intensity of 140 kt, and ACE of 1.4×10^6 kt^2 (Table 1). Within the annual MSEA-ALL-TC, there were 4.9 (52%) WNP-TC, 2.6 (27.8%) SCS-TC and 1.9 (20.2%) BoB-TC on average, which had an annual ACE of 1.0×10^6 kt^2, 0.2×10^6 kt^2 and 0.2×10^6 kt^2, respectively (Table 1). MSEA-ALL-TC characteristics showed interannual and interdecadal fluctuations, during which 1996, 2013 and 2017 are the 3 years having the largest TC numbers from 1983 to 2020 in the MSEA (Figure 2a). Meanwhile, the temporal trends of annual MSEA-ALL-TC characteristics have slopes close to zero. To investigate the influence of TCs from the three formation basins on MSEA-ALL-TC, we analysed TC characteristics originating in the three formation basins separately. As a result, the annual number, total duration, and ACE of WNP-TC and SCS-TC were significantly correlated with the corresponding characteristics of MSEA-ALL-TC, respectively (Figure 2b, c). Simultaneously, the annual number and maximum intensity of BoB-TC were also considerably associated with MSEA-ALL-TC, respectively (Figure 2d). The significant correlations indicate that TCs from the WNP, SCS and BoB strongly related to the MSEA-ALL-TC influencing the MSEA, with the highest correlation between WNP-TC and

10970088, 2023, 13, Downloaded from https://rmets.onlinelibrary.wiley.com/doi/10.1002/joc.8180, Wiley Online Library on [19/06/2024]. See the Terms and Conditions (https://onlinelibrary.wiley.com/terms-and-conditions) on Wiley Online Library for rules of use; OA articles are governed by the applicable Creative Commons License

TABLE 1 Annual mean tropical cyclone (TC) characteristics influenced Mainland Southeast Asia (MSEA) from 1983 to 2020

TC characteristics	MSEA-ALL-TC	WNP-TC	SCS-TC	BoB-TC
Annual number	9.4	4.9 (52.0%)	2.6 (27.8%)	1.9 (20.2%)
Annual total duration (hour)	538.3	244.7 (45.5%)	208.5 (38.7%)	85.1 (15.8%)
Annual maximum intensity (kt)	140.0	140.0	105.0	140.0
Annual accumulated cyclone energy (ACE, $\times 10^6$ kt^2)	1.4	1.0 (71.4%)	0.2 (14.3%)	0.2 (14.3%)

Note: The percentage represents the portion of TCs from different formation basins for each characteristic. TCs from all three basins influencing MSEA, WNP, SCS and BoB, was abbreviated as MSEA-ALL-TC, WNP-TC, SCS-TC and BoB-TC, respectively.

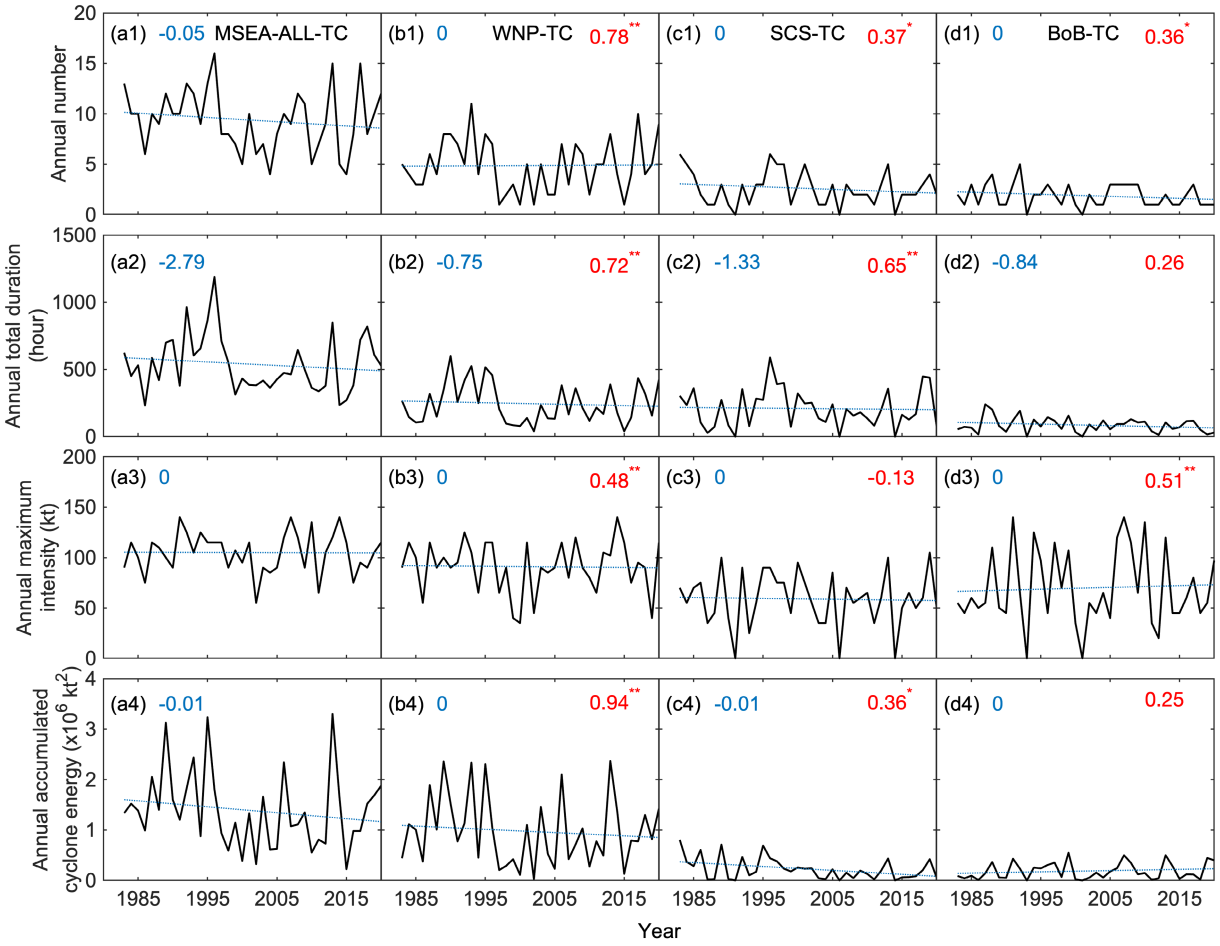

FIGURE 2 Time series of annual landfalling tropical cyclone (TC) characteristics: number (a1–d1), total duration (a2–d2), maximum intensity (a3–d3) and accumulated cyclone energy (a4–d4) in the Mainland Southeast Asia during 1983–2020. TCs originating in all three basins (MSEA-ALL-TC, a1–a4), the Western North Pacific (WNP-TC, b1–b4), the South China Sea (SCS-TC, c1–c4) and the Bay of Bengal (BoB-TC, d1–d4). The number in blue (on the upper left of each panel) is the linear trend of TC characteristics, and no linear trend is significant based on the Mann-Kendall trend test. The number in red (on the upper right of each pan) is the correlation coefficient between TC characteristics from each of the three basins and the corresponding characteristics of MSEA-ALL-TC. The significance level passed the 95% and the 99% significance level is denoted by * and **, respectively. [Colour figure can be viewed at wileyonlinelibrary.com]

MSEA-ALL-TC. Additionally, by testing the correlations between each basin's TC characteristics and TCR, the three basins' TC characteristics (number, total duration, maximum intensity and ACE) were strongly associated with their TCR, respectively (Table 2). Total duration had the highest correlation with TCR among the TC characteristics, followed by the number, ACE and maximum intensity; only the maximum intensity of MSEA-ALL-TC showed no correlation with the TCR of MSEA-ALL-TC. Therefore, MSEA-ALL-TC of the MSEA was dominated by the WNP-TC; among the TC characteristics, TCR was primarily related to the duration.

10970088, 2023, 13, Downloaded from https://rmets.onlinelibrary.wiley.com/doi/10.1002/joc.8180, Wiley Online Library on [19/06/2024]. See the Terms and Conditions (https://onlinelibrary.wiley.com/terms-and-conditions) on Wiley Online Library for rules of use; OA articles are governed by the applicable Creative Commons License

TABLE 2 Correlations between tropical cyclone (TC) characteristics from all three basins and their respective annual TC rainfall (TCR) from formation basins.

TC characteristics	TCR of MSEA-ALL-TC	TCR of WNP-TC	TCR of SCS-TC	TCR of BoB-TC
Annual number	0.70**	0.73**	0.73**	0.55**
Annual total duration	0.88**	0.84**	0.81**	0.62**
Annual maximum intensity	0.22	0.41*	0.82**	0.47**
Annual accumulated cyclone energy (ACE)	0.50**	0.62**	0.55**	0.35*

Note: TCs from all three basins influence MSEA, WNP, SCS, and BoB, was abbreviated as MSEA-ALL-TC, WNP-TC, SCS-TC and BoB-TC, respectively; the significance level passed the 95% and the 99% is denoted by * and **, respectively.

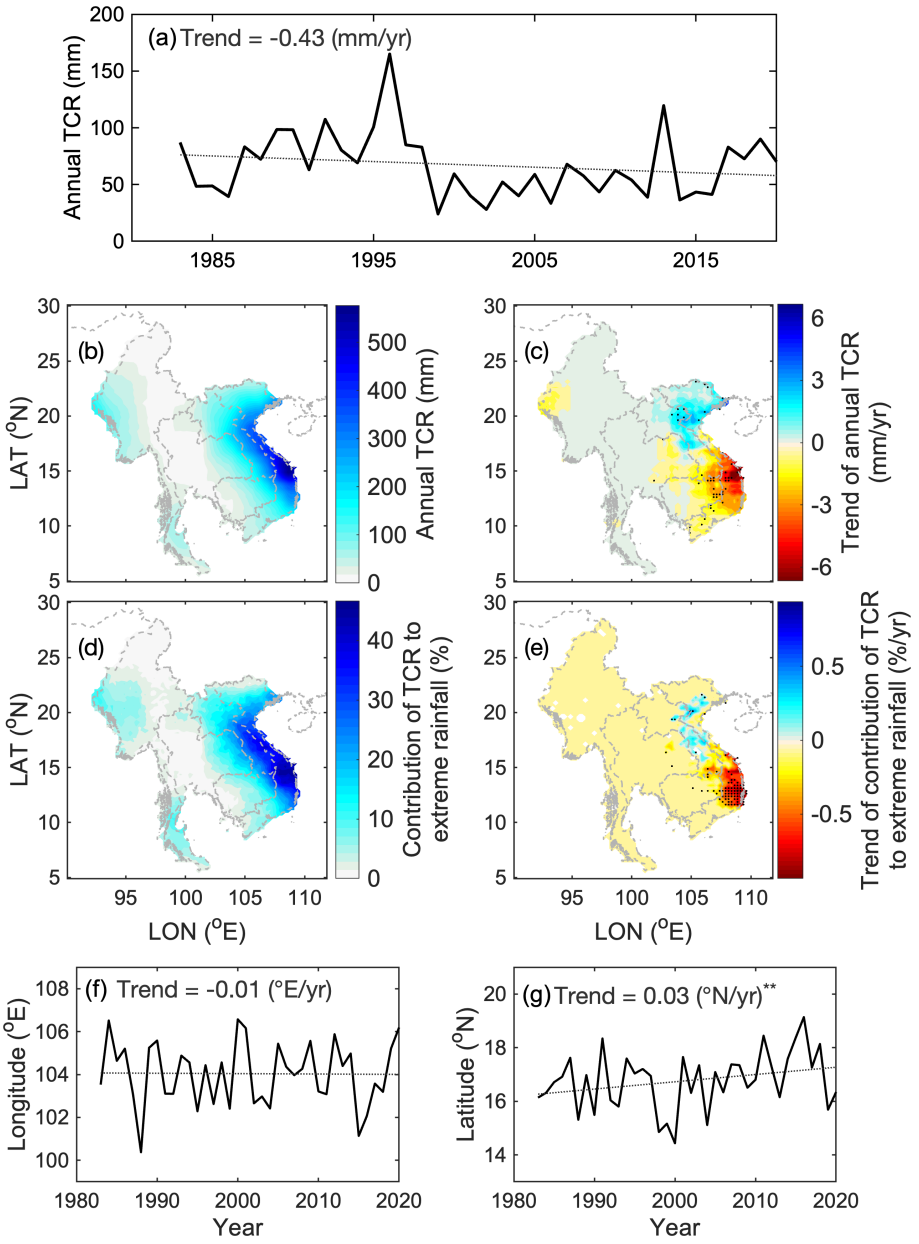

FIGURE 3 Spatiotemporal patterns of annual landfalling tropical cyclone rainfall (TCR) (a–c), its contribution to extreme rainfall (d, e), and the movements of its gravity centers (f, g) in Mainland Southeast Asia during 1983–2020. The contribution values were calculated using peak-over-threshold (POT) approaches (Khouakhi et al., 2017). The TCR center of gravity analysis along longitude and latitude refers to Koren et al. (2009). The statistically significant trend in panels c and e ($p < 0.05$) is marked by •. ** denotes the trend that passed the 99% significance level. [Colour figure can be viewed at wileyonlinelibrary.com]

10970088, 2023, 13, Downloaded from https://rmets.onlinelibrary.wiley.com/doi/10.1002/joc.8180, Wiley Online Library on [19/06/2024]. See the Terms and Conditions (https://onlinelibrary.wiley.com/terms-and-conditions) on Wiley Online Library for rules of use; OA articles are governed by the applicable Creative Commons License

3.2 | Spatiotemporal patterns of TCR in the MSEA

Generally, annual TCR in the MSEA exhibited interannual fluctuations in the temporal series of 1983–2020, averaging 67 mm per year (Figure 3a). It presents a slight negative trend during the period. On the spatial scale, the east coast of MSEA received major annual TCR with the highest value of ~577 mm, and the second center of annual TCR was shown on the west coast, where the highest value was ~159 mm (Figure 3b). Based on the trend analysis, annual TCR on the east coast showed increasing tendencies in the north of 15° N and contrarily decreasing tendencies in the south of 15° N; annual TCR on the west coast did not change substantially (Figure 3c). The contribution of TCR to extreme rainfall exhibited similar spatial patterns to the annual TCR (Figure 3d, e). The TCR held a considerable share in extreme rainfall, showing the highest contributions of ~47% and ~13% on the east and west coast in MSEA during 1983–2020, respectively (Figure 3d). Based on the center of gravity analysis, the annual TCR center in the MSEA was northward-moving at an annual rate of 0.03° N/yr but with no clear trend in the east–west direction over 1983–2020 (Figure 3f, g), which is consistent with the spatially contrasting tendencies in the east coast (Figure 3c).

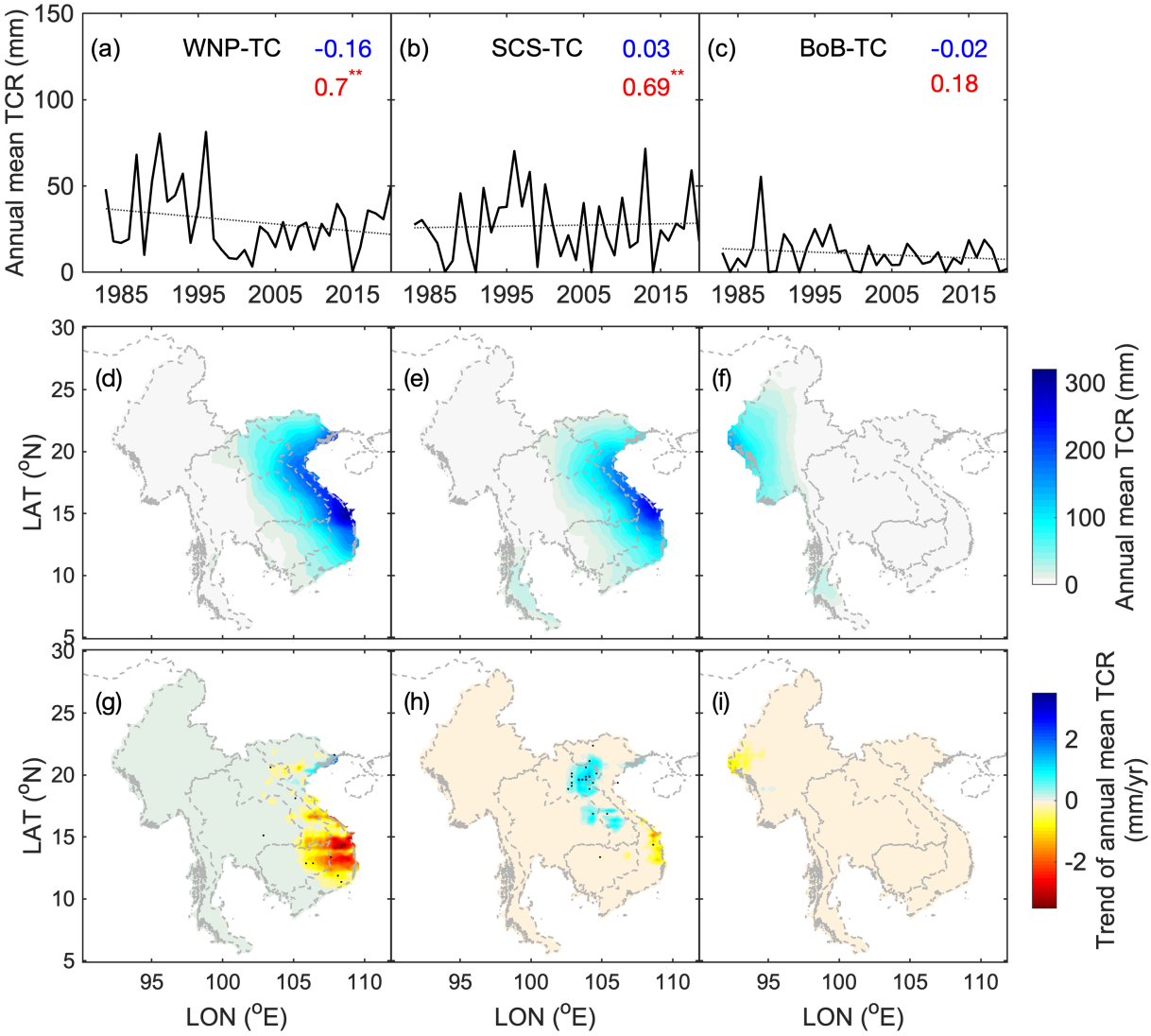

FIGURE 4 Time series and spatial distributions of landfalling tropical cyclone rainfall (TCR) over Mainland Southeast Asia from the Western North Pacific (WNP-TC, a, d, g), the South China Sea (SCS-TC, b, e, h), and the Bay of Bengal (BoB-TC, c, f, i) during 1983–2020, respectively. The number in blue in panels a–c is the linear trend of TCR, and no linear trend is significant based on the Mann–Kendall trend test. The number in red in panels a–c is the correlation coefficient between the TCR from each of the three basins and the TCR from all the basins, and the symbol of ** represents the significance level passing the 99%. The statistically significant ($p < 0.05$) trends are marked by • in panels g–i. [Colour figure can be viewed at wileyonlinelibrary.com]

10970088, 2023, 13, Downloaded from https://rmets.onlinelibrary.wiley.com/doi/10.1002/joc.8180, Wiley Online Library on [19/06/2024]. See the Terms and Conditions (https://onlinelibrary.wiley.com/terms-and-conditions) on Wiley Online Library for rules of use; OA articles are governed by the applicable Creative Commons License

3.3 | TCR from the formation basins

In the MSEA, the annual TCR of WNP-TC, SCS-TC and BoB-TC showed interannual fluctuations during 1983–2020, with trends close to zero (Figure 4a–c). The annual TCR of WNP-TC was comparable to SCS-TC but with broader spatial coverage, and the TCR of BoB-TC was relatively small. During the study period, both the TCR of WNP-TC and SCS-TC were highly correlated with the TCR of MSEA-ALL-TC ($p < 0.01$) but not for the TCR of BoB-TC. Spatially, WNP-TC and SCS-TC primarily induced TCR on the east coast, and BoB-TC mainly yielded TCR on the west coast (Figure 4d–f). Meanwhile, the TCR of WNP-TC reduced on the southeast coast, the TCR of SCS-TC increased on the northeast coast, and the TCR of BoB-TC decreased in a tiny part of the west coast (Figure 4g–i). The contrasting trends of TCR from the three formation basins were similar to the TCR of MSEA-ALL-TC (shown in Figure 3).

The mean annual TC rainfall rate of SCS-TC in MSEA during 1983–2020 (4.30 mm/day) was more prominent than WNP-TC (4.25 mm/day) and BoB-TC (2.57 mm/day) on average (Figure 5a–c). Similar to the spatial patterns of trends in TCR (see Figure 4), the TC rainfall rate of WNP-TC reduced on the southeast coast, and that of SCS-TC increased on the northeast coast (Figure 5g, h). However, unlike the

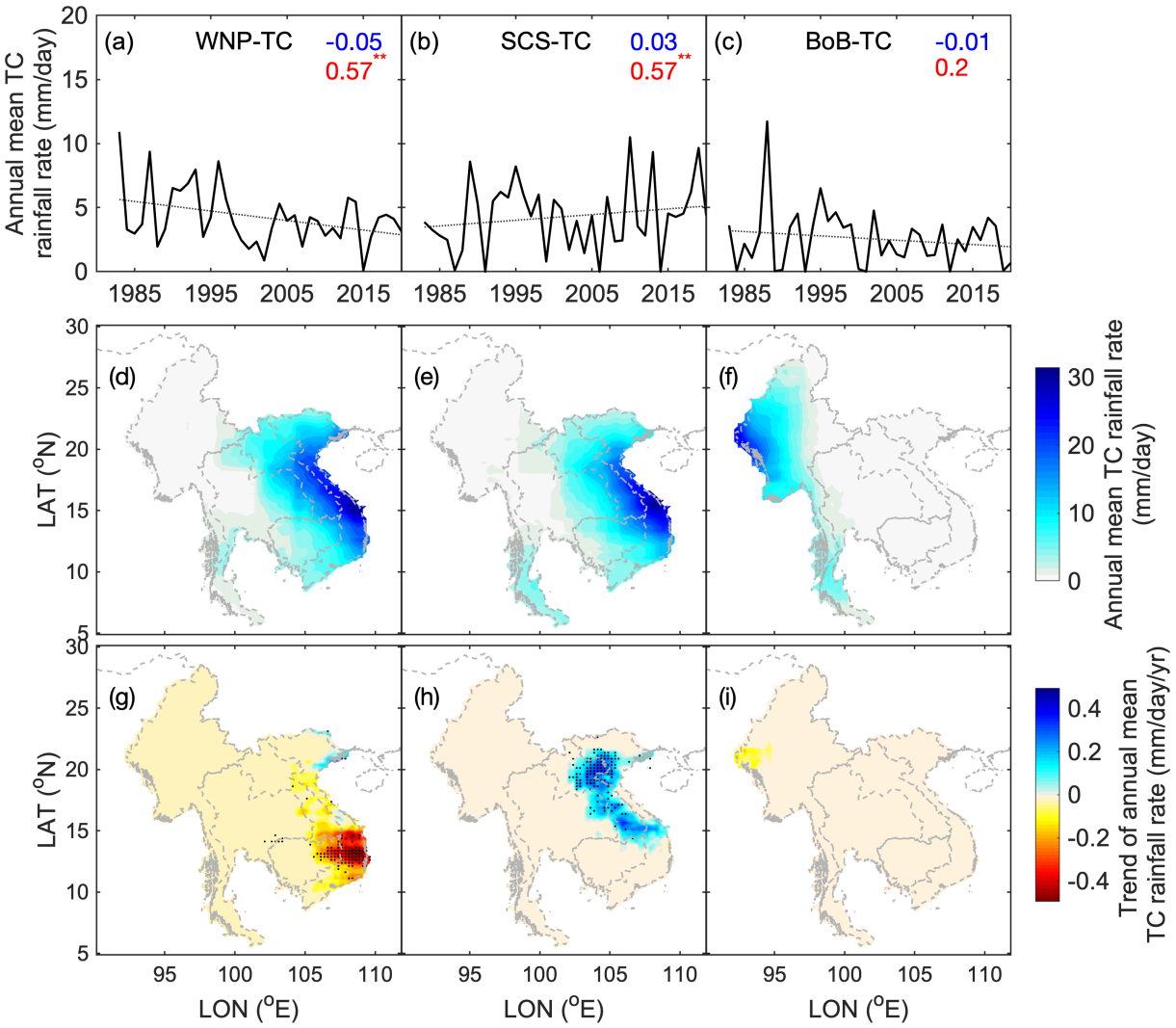

FIGURE 5 Time series and spatial distributions of landfalling tropical cyclone (TC) rainfall rate over Mainland Southeast Asia from the Western North Pacific (WNP-TC, a, d, g), the South China Sea (SCS-TC, b, e, h), and the Bay of Bengal (BoB-TC, c, f, i) during 1983–2020, respectively. The number in blue in panels a–c is the linear trend of TC rainfall rate, and no linear trend is significant based on the Mann-Kendall trend test. The number in red in panels a–c is the correlation coefficient between the TC rainfall rate from each of the three basins and the TC rainfall rate from all the basins, and the symbol of ** represents the significance level passing the 99%. The statistically significant ($p < 0.05$) trends are marked by • in panels g–i. [Colour figure can be viewed at wileyonlinelibrary.com]

10970088, 2023, 13, Downloaded from https://rmets.onlinelibrary.wiley.com/doi/10.1002/joc.8180, Wiley Online Library on [19/06/2024]. See the Terms and Conditions (https://onlinelibrary.wiley.com/terms-and-conditions) on Wiley Online Library for rules of use; OA articles are governed by the applicable Creative Commons License

spatial patterns of trends in TCR, SCS-TC had a greater spatial coverage of increasing TC rainfall rate than increasing TCR (Figures 4h and 5h), and a positive TC rainfall rate of BoB-TC occurred on the west coast (Figure 5i).

3.4 | TCD from the formation basins

The coupled spatial patterns and associated time series corresponding to MSEA-ALL-TC's TCR and TCD are displayed in Figure 6. The coupled TCR and TCD variations'

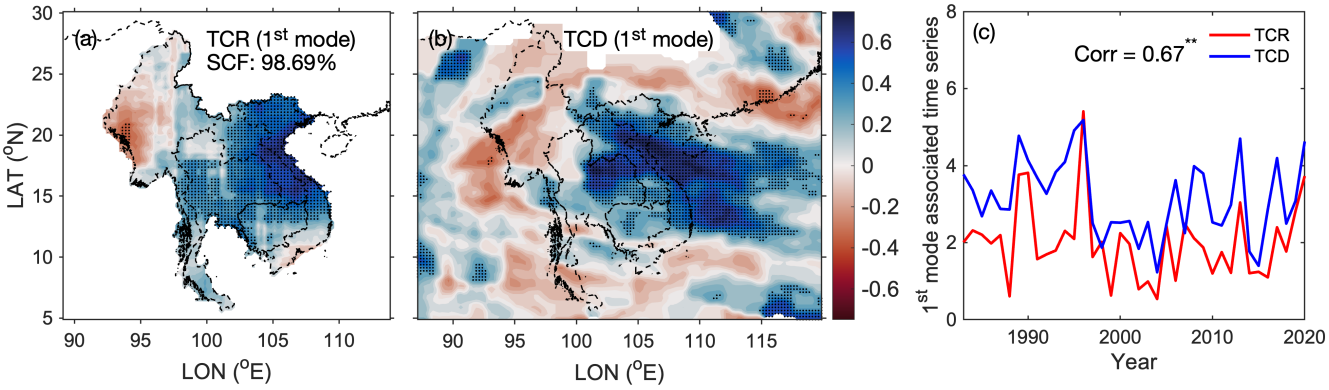

FIGURE 6 Heterogeneous correlation patterns of the first mode of the SVD analysis of annual tropical cyclone rainfall (TCR, a) and track density (TCD, b) and the associated time series during 1983–2020. The time series are normalized by the relevant standard deviation. The statistically significant ($p < 0.05$) heterogeneous correlations are marked by • in panels a–b. The square covariance fraction (SCF) of the first mode is shown in panel a. The correlation coefficient between the first mode associated time series of TCR and TCD is shown in panels c, and the symbol of ** represents the significance level passing the 99%. [Colour figure can be viewed at wileyonlinelibrary.com]

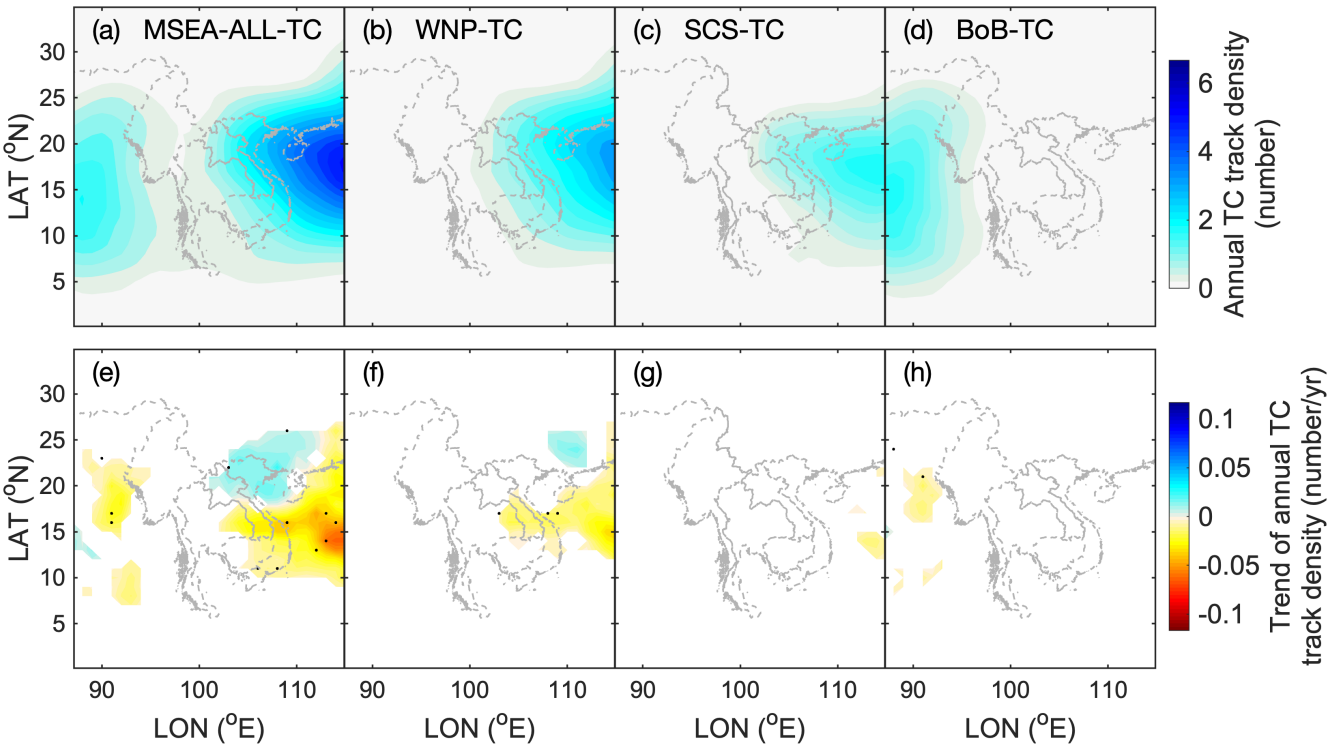

FIGURE 7 Spatial distributions of the mean and trend of annual tropical cyclone track density (TCD) that influenced Mainland Southeast Asia during 1983–2020 originating from all three basins (MSEA-ALL-TC, a, e), the Western North Pacific (WNP-TC, b, f), the South China Sea (SCS-TC, c, g) and the Bay of Bengal (BoB-TC, d, h). The statistically significant ($p < 0.05$) trends are marked by • in panels e-h. [Colour figure can be viewed at wileyonlinelibrary.com]

10970088, 2023, 13, Downloaded from https://rmets.onlinelibrary.wiley.com/doi/10.1002/joc.8180, Wiley Online Library on [19/06/2024]. See the Terms and Conditions (https://onlinelibrary.wiley.com/terms-and-conditions) on Wiley Online Library for rules of use; OA articles are governed by the applicable Creative Commons License

TABLE 3 Sen's trend of annual TC number in the south and north of 15°N of the SCS, and the annual maximum termination locations of TCs originated in the ocean basins.

TC indexes		Sen's trend	*p* value
Annual TC numbers in the south of 15°N of the SCS	WNPSCS-TC	0	1
	WNP-TC	0	0.42
	SCS-TC	0	0.72
Annual TC numbers in the north of 15°N of the SCS	WNPSCS-TC	0	0.59
	WNP-TC	0	0.50
	SCS-TC	0	0.90
Annual maximum terminated latitude of TCs originated in the ocean basins	WNPSCS-TC	−0.02	0.73
	WNP-TC	−0.03	0.76
	SCS-TC	0.04	0.56
Annual maximum terminated longitude of TCs originated in the ocean basins	WNPSCS-TC	−0.25*	0.02
	WNP-TC	−0.07	0.63
	SCS-TC	−0.08	0.72

Note: Total TCs from both WNP and SCS was abbreviated as WNPSCS-TC; TCs from WNP and SCS, was abbreviated as WNP-TC and SCS-TC, respectively. The significance level passed the 95% significance level is denoted by *.

first mode accounted for 98.69% of the total square covariance between them. The first mode exhibited a strong and highly significant coupling between TCR and TCD, with a significant correlation coefficient between the associated time series. Furthermore, there were positive and significant impacts of TCD on TCR in most areas, whereas the negative effects of TCD variation exist in a small part of western Myanmar (Figure 6a). On the other hand, the significant positive correlations between the TCD's first mode and the TCR's first mode-associated time series indicated that the TCD in the SCS and the eastern and southern MSEA were key areas influencing the TCR (Figure 6b). This TCD mainly originated from the WNP and SCS. In addition, both time series were dominated by interdecadal fluctuations (Figure 6c). Overall, the results show that the TCR and TCD are strongly coupled.

Spatial patterns of annual TCD of MSEA-ALL-TC presented a higher density in the east side ocean of MSEA than in the west side, indicating higher TC track frequency in the SCS than in the BoB (Figure 7a). Long-term trend analysis revealed reduced TCD in some parts of the SCS and the BoB and increasing trends in the northern SCS (Figure 7e). This pattern is consistent with the trend of the annual TCR of MSEA-ALL-TC (Figure 3c). We then separately analysed the TCD of the formation basins. Results showed that the reduced TCD of MSEA-ALL-TC is consistent with the diminished WNP-TC in the SCS, and BoB-TC in the BoB (Figure 7f–h), but no clear trend was found for the TCD of SCS-TC (Figure 7g). The positive trend of TCD is attributed to the significant westward trend of the TC tracks in the north of SCS. Specifically, we found the annual maximum terminated longitude of the total TCs from both WNP and SCS had a significant westward trend, even though it is insignificant for either WNP-TC or SCS-TC (Table 3). Overall, the results indicate that the reduced TCD of WNP-TC and BoB-TC is associated with the spatiotemporal change of annual TCR in the MSEA.

4 | DISCUSSION

4.1 | TC characteristics and association with TCR in MSEA

TC activities in the formation basins had large interannual and interdecadal variabilities, which were strongly associated with large-scale environment, such as shifts in the Pacific Decadal Oscillation, the Intertropical Convergence Zone (Basconcillo & Moon, 2021; Goh & Chan, 2010; Jiang & Zipser, 2010; Nguyen-Thi et al., 2012) and the El Niño–Southern Oscillation (Balaguru et al., 2016; Elsner & Liu, 2003; Wang et al., 2020; Zhang, Gu, et al., 2018). Although experiencing large fluctuations, TC characteristics from the three formation basins presented insignificant tendencies during 1983–2020. Many studies have reported a north-westward shift of TC tracks in the WNP, implying fewer TCs formed in WNP moving into SCS (Knutson et al., 2020; Liu, Chan, & Kubota, 2021; Park et al., 2014). However, we did not find an apparent tendency of WNP-TC to influence the MSEA during the study period. Therefore, the impact of the shifting TC track requires further analysis.

Different formation basins' TCs influenced the MSEA unequally. Among the three basins, WNP-TC contributed 52% of the MSEA-ALL-TC number, followed by SCS-TC

10970088, 2023, 13, Downloaded from https://rmets.onlinelibrary.wiley.com/doi/10.1002/joc.8180, Wiley Online Library on [19/06/2024]. See the Terms and Conditions (https://onlinelibrary.wiley.com/terms-and-conditions) on Wiley Online Library for rules of use; OA articles are governed by the applicable Creative Commons License

(27.8%) and BoB-TC (22.2%), showing the dominant role of WNP-TC in MSEA (Chen et al., 2019). TC characteristics (including number, total duration and ACE) of WNP-TC and SCS-TC correlated with the MSEA-ALL-TC's corresponding characteristics (see Figure 2). Meanwhile, the annual number and maximum intensity of BoB-TC have significant correlations with the MSEA-ALL-TC. Moreover, leading by total duration, the TC characteristics of the three basins were strongly associated with their TCR, respectively (Table 2). This result agrees with previous studies revealing a close relationship between TCR and TC duration (Chen et al., 2019; Cheung et al., 2018; Lonfat et al., 2004; Zhang, Villarini, et al., 2018). Some studies indicated that TC intensity is correlated with TCR parameters (Kim et al., 2006; Yu et al., 2017). We also found significant correlations between these formation basins' maximum intensity and TCR, but not for the MSEA-ALL-TC in the multi-TC-source MSEA (Chen et al., 2019; Park et al., 2011).

After separating the TCR from the three formation basins, we found that the mean contributions of TCR from these basins to MSEA-ALL-TC's TCR was about 43.5% (WNP-TC), 39.1% (SCS-TC) and 17.4% (BoB-TC), respectively (see Figure 4). Furthermore, the portions of the basins were closely linked to their shares of the total duration, which were 45.5% (WNP-TC), 38.7% (SCS-TC) and 15.8% (BoB-TC) (see Table 1), respectively. These results again indicated a strong association between the total duration and TCR. On the other hand, it also suggested high TCR induced by the smaller number of the SCS-TC compared with the WNP-TC (see Table 1). Moreover, SCS-TC has a higher rainfall rate than the WNP-TC and BoB-TC. Furthermore, the increasing SCS-TC rainfall rate in the northeast indicates higher extreme rainfall risks in MSEA.

4.2 | Spatiotemporal pattern of TCR in MSEA

TCR contributed about 7% (67 mm) to annual total rainfall at the regional scale of the MSEA during 1983–2020. It contributed considerably to extreme rainfall (Chhin et al., 2016; Nguyen-Thi et al., 2012), which was up to 47% based on our results. The high contributions of TCR to extreme rainfall also occurred in other TC landfalling areas (Chang et al., 2012; Jiang et al., 2011; Khouakhi et al., 2017). In East Asia, Australia, the USA and Mexico, TCR contributed 35–50% to annual total rainfall (Cheung et al., 2018; Khouakhi et al., 2017), and it could account for up to 60% of the monthly rainfall in the WNP (Chen & Fu, 2015; Kubota & Wang, 2009). Both annual total and extreme TCR were concentrated in the east of MSEA (Figure 3), induced by the WNP-TC and SCS-TC.

Changes in the TCR were related to TC rainfall rate and TCD. We found that the annual TC rainfall rate of WNP-TC decreased in the southeast of MSEA, but the annual TC rainfall rate of SCS-TC increased in the northeast of MSEA over the study period (Figures 4 and 5). These patterns feature the contrasting changes in tendencies of the annual TCR of MSEA-ALL-TC (Figure 3). Thus, changes in the TCR of MSEA-ALL-TC were attributed to the TC rainfall rate changes of WNP-TC and SCS-TC. On the other hand, the SVD analysis revealed that the reduction of TCD in the southern part of SCS was from WNP-TC (Figures 6 and 7), indicating the influence of TCD from WNP-TC on the reduced TCR in southeast MSEA (Chen et al., 2019; Lonfat et al., 2004; Park et al., 2014). Existing studies also found that decreased TCD has reduced TCR in southern China (Chang et al., 2012; Cheung et al., 2018). However, the insignificant trend of TCD of SCS-TC (Figure 7g) indicates little influence of TCD change on the increasing TCR in the northeast of MSEA, which may be primarily attributed to the rising SCS-TC rainfall rate (Figure 5b, h). Taken together, the contrasting climatology of TCR in MSEA was mainly the joint influence of changes in the track density of WNP-TC, and the rainfall rate of SCS-TC. The authors plan to conduct another study focusing on the driving factors of the increasing TC rainfall rate.

TCR in the MSEA has substantially influenced the region (Chen, Giese, & Chen, 2020; Hu et al., 2018; Osti & Nakasu, 2016; Peduzzi et al., 2012; Pielke et al., 2008), and future changes in the large-scale environment are projected to increase the TC intensity and rainfall rate (Chen, Emanuel, et al., 2020; Knutson et al., 2010, 2020; Sobel et al., 2016). Representative estimation projected that the future TC rainfall rate would increase at the rate of ~7% per 1°C of global warming (Knutson et al., 2020). In addition, previous studies have emphasized slowdown translation speeds and decaying trends of TCs under global warming, which make TCs linger in the landfalling area (Knutson et al., 2020; Li & Chakraborty, 2020), for example in South China (Tran et al., 2022). The TC activity could substantially increase the TCR since the TC duration is the most correlated with TCR, implying that future TCR and the associated impacts could be more significant than the historical level. Therefore, more attention should be paid to mitigating the potential effects of TCs.

5 | CONCLUSIONS

This study took the TC-prone MSEA as the study area to investigate the TCR from the three formation basins

10970088, 2023, 13, Downloaded from https://rmets.onlinelibrary.wiley.com/doi/10.1002/joc.8180, Wiley Online Library on [19/06/2024]. See the Terms and Conditions (https://onlinelibrary.wiley.com/terms-and-conditions) on Wiley Online Library for rules of use; OA articles are governed by the applicable Creative Commons License

related to TC characteristics during 1983–2020. For the whole of MSEA, up to 47% of the annual extreme rainfall amount was contributed by the total TCR. TCs originating from the WNP and the SCS more substantially influenced the interannual variability of the total TCs and the associated rainfall in the study region than the TCs developed from the BoB. Spatially contrasting trends of TCR that occurred in the eastern MSEA were related to the changes in TCD. Specifically, the significant decreasing trends of TCR in the southeast study region were associated with the reduced TCD originating from the WNP. In contrast, the increasing trends of TCR in the northeast study region dominated by the increased rainfall rate of TCs originating from the SCS. In addition, we found that TCs from the SCS generated a higher rainfall rate than those from the WNP and the BoB. TC characteristics (such as total duration, number, accumulated cyclone energy and maximum intensity) were correlated with the TCR from their source basins. The total duration has the highest correlation, suggesting the potential risk of slowdown cyclone translation speed. Our results provide a more in-depth understanding of TCR changes and the relationship with cyclone characteristics in multi-sourcing TC landfalling regions, and support regional TC-associated risk assessment and possible mitigation and adaptation to future climate change.

AUTHOR CONTRIBUTIONS

Aifang Chen: Conceptualization; methodology; investigation; funding acquisition; writing – original draft; writing – review and editing; visualization. **Hao Huang:** Conceptualization; visualization; writing – review and editing. **Jie Wang:** Methodology; writing – review and editing; formal analysis. **Yuxin Li:** Visualization; writing – review and editing. **Deliang Chen:** Supervision; writing – review and editing; funding acquisition; formal analysis. **Junguo Liu:** Supervision; funding acquisition; writing – review and editing; project administration; conceptualization.

ACKNOWLEDGEMENTS

We thank Dr. Ping Lu for her constructive comments. This research was supported by the National Natural Science Foundation of China (Grant No. 42101041, 91537210), the China Postdoctoral Science Foundation (Grant No. 2021M691403), the Strategic Priority Research Program of the Chinese Academy of Sciences (Grant No. XDA20060402, XDA20060401), the Swedish STINT (Grant No. CH2019-8377), and the SUSTech Presidential Postdoctoral Fellowship. It was also partly supported by the Henan Provincial Key Laboratory of Hydrosphere and Watershed Water Security.

CONFLICT OF INTEREST STATEMENT

The authors declare no conflicts of interest.

DATA AVAILABILITY STATEMENT

The datasets presented for this study can be found in the latest International Best Track Archive for Climate Stewardship (https://www.ncdc.noaa.gov/ibtracs/), the Precipitation Estimation from Remotely Sensed Information using Artificial Neural Networks-Climate Data Record (PERSIANN-CDR, https://www.ncdc.noaa.gov/cdr/atmospheric/precipitation-persiann-cdr).

ORCID

Aifang Chen https://orcid.org/0000-0002-3237-3122
Deliang Chen https://orcid.org/0000-0003-0288-5618

REFERENCES

Ashouri, H., Hsu, K.L., Sorooshian, S., Braithwaite, D.K., Knapp, K.R., Cecil, L.D. et al. (2015) PERSIANN-CDR: daily precipitation climate data record from multisatellite observations for hydrological and climate studies. *Bulletin of the American Meteorological Society*, 96(1), 69–83. Available from: https://doi.org/10.1175/BAMS-D-13-00068.1

Bakkensen, L.A., Park, D.S.R. & Sarkar, R.S.R. (2018) Climate costs of tropical cyclone losses also depend on rain. *Environmental Research Letters*, 13(7), 074034. Available from: https://doi.org/10.1088/1748-9326/aad056

Balaguru, K., Leung, L.R., Lu, J. & Foltz, G.R. (2016) Ameridional dipole in premonsoon bay of bengal tropical cyclone activity induced by ENSO. *Journal of Geophysical Research*, 121(12), 6954–6968. Available from: https://doi.org/10.1002/2016JD024936

Basconcillo, J. & Moon, I.J. (2021) Recent increase in the occurrences of Christmas typhoons in the Western North Pacific. *Scientific Reports*, 11(1), 1–10. Available from: https://doi.org/10.1038/s41598-021-86814-x

Bell, G.D., Halpert, M.S., Schnell, R.C., Higgins, R.W., Lawrimore, J., Kousky, V.E. et al. (2000) Climate assessment for 1999. *Bulletin of the American Meteorological Society*, 81(6), 1328. Available from: https://doi.org/10.1175/1520-0477(2000)081<1328:caf>2.3.co;2

Bretherton, C.S., Smith, C. & Wallace, J.M. (1992) An intercomparison of methods for finding coupled patterns in climate data. *Journal of Climate*, 5, 541–560. Available from: https://doi.org/10.1175/1520-0442(1992)005<0541:AIOMFF>2.0.CO;2

Camargo, S.J. & Sobel, A.H. (2005) Western North Pacific tropical cyclone intensity and ENSO. *Journal of Climate*, 18(15), 2996–3006. Available from: https://doi.org/10.1175/JCLI3457.1

Chang, C.P., Lei, Y., Sui, C.H., Lin, X. & Ren, F. (2012) Tropical cyclone and extreme rainfall trends in east Asian summer monsoon since mid-20th century. *Geophysical Research Letters*, 39(18). Available from: https://doi.org/10.1029/2012GL052945

Chen, A., Chen, D. & Azorin-Molina, C. (2018) Assessing reliability of precipitation data over the Mekong River basin: a comparison of ground-based, satellite, and reanalysis datasets. *International Journal of Climatology*, 1–21, 4314–4334. Available from: https://doi.org/10.1002/joc.5670

10970088, 2023, 13, Downloaded from https://rmets.onlinelibrary.wiley.com/doi/10.1002/joc.8180, Wiley Online Library on [19/06/2024]. See the Terms and Conditions (https://onlinelibrary.wiley.com/terms-and-conditions) on Wiley Online Library for rules of use; OA articles are governed by the applicable Creative Commons License

Chen, A., Emanuel, K.A., Chen, D., Lin, C. & Zhang, F. (2020) Rising future tropical cyclone-induced extreme winds in the Mekong River basin. *Science Bulletin*, 65(5), 419–424. Available from: https://doi.org/10.1016/j.scib.2019.11.022

Chen, A., Giese, M. & Chen, D. (2020) Flood impact on mainland Southeast Asia between 1985 and 2018: The role of tropical cyclones. *Journal of Flood Risk Management*, 13(2), 1–13. Available from: https://doi.org/10.1111/jfr3.12598

Chen, A., Ho, C.H., Chen, D. & Azorin-Molina, C. (2019) Tropical cyclone rainfall in the Mekong River basin for 1983–2016. *Atmospheric Research*, 226, 66–75. Available from: https://doi.org/10.1016/j.atmosres.2019.04.012

Chen, F.J. & Fu, Y.F. (2015) Contribution of tropical cyclone rainfall at categories to total precipitation over the Western North Pacific from 1998 to 2007. *Science China Earth Sciences*, 58(11), 2015–2025. Available from: https://doi.org/10.1007/s11430-015-5103-9

Cheung, K., Yu, Z., Elsberry, R.L., Bell, M., Jiang, H., Lee, T.C. et al. (2018) Recent advances in research and forecasting of tropical cyclone rainfall. *Tropical Cyclone Research and Review*, 7(2), 106–127. Available from: https://doi.org/10.6057/2018TCRR02.03

Chhin, R., Trilaksono, N.J. & Hadi, T.W. (2016) Tropical cyclone rainfall structure affecting indochina peninsula and lower mekong river basin (LMB). *Journal of Physics: Conference Series*, 739(1), 12103. Available from: https://doi.org/10.1088/1742-6596/739/1/012103

Choi, W., Ho, C.H., Kim, J. & Chan, J.C.L. (2019) Near-future tropical cyclone predictions in the western North Pacific: fewer tropical storms but more typhoons. *Climate Dynamics*, 53(3–4), 1341–1356. Available from: https://doi.org/10.1007/s00382-019-04647-x

Elsner, J.B. & Liu, K.B. (2003) Examining the ENSO-typhoon hypothesis. *Climate Research*, 25(1), 43–54. Available from: https://doi.org/10.3354/cr025043

Emanuel, K. (2005) Increasing destructiveness of tropical cyclones over the past 30 years. *Nature*, 436(7051), 686–688. Available from: https://doi.org/10.1038/nature03906

Fudeyasu, H., Hirose, S., Yoshioka, H., Kumazawa, R. & Yamasaki, S. (2014) A global view of the landfall characteristics of tropical cyclones. *Tropical Cyclone Research and Review*, 3(3), 178–192. Available from: https://doi.org/10.6057/2014TCRR03.04

Goh, A.Z.C. & Chan, J.C.L. (2010) Interannual and interdecadal variations of tropical cyclone activity in the South China Sea. *International Journal of Climatology*, 30(6), 827–843. Available from: https://doi.org/10.1002/joc.1943

Hoarau, K., Bernard, J. & Chalonge, L. (2012) Intense tropical cyclone activities in the northern Indian Ocean. *International Journal of Climatology*, 32(13), 1935–1945. Available from: https://doi.org/10.1002/joc.2406

Hu, P., Zhang, Q., Shi, P., Chen, B. & Fang, J. (2018) Flood-induced mortality across the globe: spatiotemporal pattern and influencing factors. *Science of the Total Environment*, 643, 171–182. Available from: https://doi.org/10.1016/j.scitotenv.2018.06.197

Huang, A., Zhao, Y., Zhou, Y., Yang, B., Zhang, L., Dong, X. et al. (2016) Evaluation of multisatellite precipitation products by use of ground-based data over China. *Journal of Geophysical Research*, 121(18), 10654–10675. Available from: https://doi.org/10.1002/2016JD025456

Jiang, H., Liu, C. & Zipser, E.J. (2011) A TRMM-based tropical cyclone cloud and precipitation feature database. *Journal of Applied Meteorology and Climatology*, 50(6), 1255–1274. Available from: https://doi.org/10.1175/2011JAMC2662.1

Jiang, H. & Zipser, E.J. (2010) Contribution of tropical cyclones to the global precipitation from eight seasons of TRMM data: regional, seasonal, and interannual variations. *Journal of Climate*, 23(6), 1526–1543. Available from: https://doi.org/10.1175/2009JCLI3303.1

Kendall, M.G. (1938) A new measure of rank correlation. *Biometrika*, 30(1/2), 81. Available from: https://doi.org/10.2307/2332226

Khouakhi, A., Villarini, G. & Vecchi, G.A. (2017) Contribution of tropical cyclones to rainfall at the global scale. *Journal of Climate*, 30, 359–372. Available from: https://doi.org/10.1175/JCLI-D-16-0298.s1

Kim, J.H., Ho, C.H., Lee, M.H., Jeong, J.H. & Chen, D. (2006) Large increase in heavy rainfall associated with tropical cyclone landfalls in Korea after the late 1970s. *Geophysical Research Letters*, 33(18), 1–5. Available from: https://doi.org/10.1029/2006GL027430

Knapp, K.R., Kruk, M.C., Levinson, D.H., Diamond, H.J. & Neumann, C.J. (2010) The international best track archive for climate stewardship (Ibtracs) unifying tropical cyclone data. *Bulletin of the American Meteorological Society*, 91(3), 362. Available from: https://doi.org/10.1175/2009BAMS2755.1

Knutson, T., Camargo, S.J., Chan, J.C.L., Emanuel, K., Ho, C.H., Kossin, J. et al. (2020) Tropical cyclones and climate change assessment part II: projected response to anthropogenic warming. *Bulletin of the American Meteorological Society*, 101(3), E303–E322. Available from: https://doi.org/10.1175/BAMS-D-18-0194.1

Knutson, T.R., McBride, J.L., Chan, J., Emanuel, K., Holland, G., Landsea, C. et al. (2010) Tropical cyclones and climate change. *Nature Geoscience*, 3(3), 157–163. Available from: https://doi.org/10.1038/ngeo779

Koren, I., Altaratz, O., Feingold, G., Levin, Z. & Reisin, T. (2009) Cloud's center of gravity-a compact approach to analyze convective cloud development. *Atmospheric Chemistry and Physics*, 9(1), 155–161. Available from: https://doi.org/10.5194/acp-9-155-2009

Kubota, H. & Wang, B. (2009) How much do tropical cyclones affect seasonal and interannual rainfall variability over the western North Pacific? *Journal of Climate*, 22(20), 5495–5510. Available from: https://doi.org/10.1175/2009JCLI2646.1

Lee, T.C., Leung, C.Y.Y., Kok, M.H. & Chan, H.S. (2012) The long term variations of tropical cyclone activity in the South China Sea and the vicinity of Hong Kong. *Tropical Cyclone Research and Review*, 1, 277–292. Available from: https://doi.org/10.6057/2012TCRR02.01

Li, L. & Chakraborty, P. (2020) Slower decay of landfalling hurricanes in a warming world. *Nature*, 587(7833), 230–234. Available from: https://doi.org/10.1038/s41586-020-2867-7

Liu, J., Chen, D., Mao, G., Irannezhad, M. & Pokhrel, Y. (2022) Past and future changes in climate and water resources in the Lancang–Mekong River basin: current understanding and future research directions. *Engineering*, 13, 144–152. Available from: https://doi.org/10.1016/j.eng.2021.06.026

10970088, 2023, 13, Downloaded from https://rmets.onlinelibrary.wiley.com/doi/10.1002/joc.8180, Wiley Online Library on [19/06/2024]. See the Terms and Conditions (https://onlinelibrary.wiley.com/terms-and-conditions) on Wiley Online Library for rules of use; OA articles are governed by the applicable Creative Commons License

Liu, K.S., Chan, J.C.L. & Kubota, H. (2021) Meridional oscillation of tropical cyclone activity in the western North Pacific during the past 110 years. *Climatic Change*, 164(1), 23. Available from: https://doi.org/10.1007/s10584-021-02983-8

Liu, L. & Wang, Y. (2020) Trends in landfalling tropical cyclone-induced precipitation over China. *Journal of Climate*, 33(6), 2223–2235. Available from: https://doi.org/10.1175/JCLI-D-19-0693.1

Liu, X., Yang, T., Hsu, K., Liu, C. & Sorooshian, S. (2017) Evaluating the streamflow simulation capability of PERSIANN-CDR daily rainfall products in two river basins on the Tibetan plateau. *Hydrology and Earth System Sciences*, 21(1), 169–181. Available from: https://doi.org/10.5194/hess-21-169-2017

Lonfat, M., Marks Jr, F.D. & Chen, S.S. (2004) Precipitation distribution in tropical cyclones using the tropical rainfall measuring Mission (TRMM) microwave imager: A global perspective. *Monthly Weather Review*, 132(7), 1645–1660.

Mei, W. & Xie, S.P. (2016) Intensification of landfalling typhoons over the Northwest Pacific since the late 1970s. *Nature Geoscience*, 9(10), 753–757. Available from: https://doi.org/10.1038/ngeo2792

Murakami, H., Delworth, T.L., Cooke, W.F., Zhao, M., Xiang, B. & Hsu, P.C. (2020) Detected climatic change in global distribution of tropical cyclones. *Proceedings of the National Academy of Sciences of the United States of America*, 117(20), 10706–10714.

Nguyen-Thi, H.A., Matsumoto, J., Ngo-Duc, T. & Endo, N. (2012) A climatological study of tropical cyclone rainfall in Vietnam. *Solaiat*, 8, 41–44. Available from: https://doi.org/10.2151/sola.2012-011

Osti, R. & Nakasu, T. (2016) Lessons learned from southern and eastern Asian urban floods: from a local perspective. *Journal of Flood Risk Management*, 9(1), 22–35. Available from: https://doi.org/10.1111/jfr3.12107

Park, D.S.R., Ho, C.H. & Kim, J.H. (2014) Growing threat of intense tropical cyclones to East Asia over the period 1977-2010. *Environmental Research Letters*, 9(1), 014008. Available from: https://doi.org/10.1088/1748-9326/9/1/014008

Park, D.S.R., Ho, C.H., Kim, J.H. & Kim, H.S. (2011) Strong landfall typhoons in Korea and Japan in a recent decade. *Journal of Geophysical Research Atmospheres*, 116(7), 1–11. Available from: https://doi.org/10.1029/2010JD014801

Peduzzi, P., Chatenoux, B., Dao, H., de Bono, A., Herold, C., Kossin, J. et al. (2012) Global trends in tropical cyclone risk. *Nature Climate Change*, 2(4), 289–294. Available from: https://doi.org/10.1038/nclimate1410

Pielke, J., Roger, A., Gratz, J., Landsea, C.W., Collins, D., Saunders, M.A. et al. (2008) Normalized hurricane damage in the United States: 1900–2005. *Natural Hazards Review*, 9, 29–42. Available from: https://doi.org/10.1061/(ASCE)1527-6988(2008)9:1(29)

Rappaport, E.N. (2014) Fatalities in the United States from Atlantic tropical cyclones: new data and interpretation. *Bulletin of the American Meteorological Society*, 95(3), 341–346. Available from: https://doi.org/10.1175/BAMS-D-12-00074.1

Sen, P.K. (1968) Estimates of the regression coefficient based on Kendall's tau. *Journal of the American Statistical Association*, 63(324), 1379–1389. Available from: https://doi.org/10.1080/01621459.1968.10480934

Skok, G., Bacmeister, J. & Tribbia, J. (2013) Analysis of tropical cyclone precipitation using an object-based algorithm. *Journal of Climate*, 26(8), 2563–2579. Available from: https://doi.org/10.1175/JCLI-D-12-00135.1

Sobel, A.H., Camargo, S.J., Hall, T.M., Lee, C.-Y., Tippett, M.K., Wing, A.A. et al. (2016) Human influence on tropical cyclone intensity. *Science*, 353(6296), 242–246.

Sobel, A.H., Wing, A.A., Camargo, S.J., Patricola, C.M., Vecchi, G.A., Lee, C.Y. et al. (2021) Tropical cyclone frequency. *Earth's Futures*, 9(12), e2021EF002275. Available from: https://doi.org/10.1029/2021EF002275

Sorooshian, S., Hsu, K.L., Gao, X., Gupta, H.V., Imam, B. & Braithwaite, D. (2000) Evaluation of PERSIANN system satellite-based estimates of tropical rainfall. *Bulletin of the American Meteorological Society*, 81(9), 2035–2046. Available from: https://doi.org/10.1175/1520-0477(2000)081<2035:EOPSSE>2.3.CO;2

Takahashi, H.G. & Yasunari, T. (2008) Decreasing trend in rainfall over Indochina during the late summer monsoon: impact of tropical cyclones. *Journal of the Meteorological Society of Japan*, 86(3), 429–438.

Tran, T.L., Ritchie, E.A. & Perkins-Kirkpatrick, S.E. (2022) A 50-year tropical cyclone exposure climatology in Southeast Asia. *Journal of Geophysical Research: Atmospheres*, 127(4), e2021jd036301. Available from: https://doi.org/10.1029/2021jd036301

Vosper, E.L., Mitchell, D.M. & Emanuel, K. (2020) Extreme hurricane rainfall affecting the Caribbean mitigated by the Paris agreement goals. *Environmental Research Letters*, 15(10), 104053. Available from: https://doi.org/10.1088/1748-9326/ab9794

Walsh, K.J.E., Mcbride, J.L., Klotzbach, P.J., Balachandran, S., Camargo, S.J., Holland, G. et al. (2016) Tropical cyclones and climate change. *Wiley Interdisciplinary Reviews: Climate Change*, 7(1), 65–89. Available from: https://doi.org/10.1002/wcc.371

Wang, B., Yang, Y., Ding, Q.H., Murakami, H. & Huang, F. (2010) Climate control of the global tropical storm days (1965–2008). *Geophysical Research Letters*, 37(7), 1–5. Available from: https://doi.org/10.1029/2010GL042487

Wang, G., Su, J., Ding, Y. & Chen, D. (2007) Tropical cyclone genesis over the South China Sea. *Journal of Marine Systems*, 68(3–4), 318–326. Available from: https://doi.org/10.1016/j.jmarsys.2006.12.002

Wang, L., Yang, Z., Gu, X. & Li, J. (2020) Linkages between tropical cyclones and extreme precipitation over China and the role of ENSO. *International Journal of Disaster Risk Science*, 11(4), 538–553. Available from: https://doi.org/10.1007/s13753-020-00285-8

Wang, S. & Toumi, R. (2021) Recent migration of tropical cyclones toward coasts. *Science*, 371, 514–517. Available from: https://doi.org/10.1126/science.abb9038

Weinkle, J., Maue, R. & Pielke, R. (2012) Historical global tropical cyclone landfalls. *Journal of Climate*, 25(13), 4729–4735. Available from: https://doi.org/10.1175/JCLI-D-11-00719.1

Yu, Z., Wang, Y., Xu, H., Davidson, N., Chen, Y., Chen, Y. et al. (2017) On the relationship between intensity and rainfall distribution in tropical cyclones making landfall over China. *Journal of Applied Meteorology and Climatology*, 56(10), 2883–2901. Available from: https://doi.org/10.1175/JAMC-D-16-0334.1

Zhang, J., Wu, L., Ren, F. & Cui, X. (2013) Changes in tropical cyclone rainfall in China. *Journal of the Meteorological Society of Japan*, 91(5), 585–595. Available from: https://doi.org/10.2151/jmsj.2013-502

10970088, 2023, 13, Downloaded from https://rmets.onlinelibrary.wiley.com/doi/10.1002/joc.8180, Wiley Online Library on [19/06/2024]. See the Terms and Conditions (https://onlinelibrary.wiley.com/terms-and-conditions) on Wiley Online Library for rules of use; OA articles are governed by the applicable Creative Commons License

Zhang, Q., Gu, X., Li, J., Shi, P. & Singh, V.P. (2018) The impact of tropical cyclones on extreme precipitation over coastal and inland areas of China and its association to ENSO. *Journal of Climate*, 31(5), 1865–1880. Available from: https://doi.org/10.1175/JCLI-D-17-0474.1

Zhang, W., Villarini, G., Vecchi, G.A. & Smith, J.A. (2018) Urbanization exacerbated the rainfall and flooding caused by hurricane Harvey in Houston. *Nature*, 563(7731), 384–388. Available from: https://doi.org/10.1038/s41586-018-0676-z

How to cite this article: Chen, A., Huang, H., Wang, J., Li, Y., Chen, D., & Liu, J. (2023). An analysis of the spatial variation of tropical cyclone rainfall trends in Mainland Southeast Asia. *International Journal of Climatology*, *43*(13), 5912–5926. https://doi.org/10.1002/joc.8180

10970088, 2023, 13, Downloaded from https://rmets.onlinelibrary.wiley.com/doi/10.1002/joc.8180, Wiley Online Library on [19/06/2024]. See the Terms and Conditions (https://onlinelibrary.wiley.com/terms-and-conditions) on Wiley Online Library for rules of use; OA articles are governed by the applicable Creative Commons License